Ann. Rev. Fluid Mech. 1981. 13:399-423

CUP, PROPELLER, VANE, AND SONIC ANEMOMETERS IN TURBULENCE RESEARCH

*8182

J. C. Wyngaard
National Center for Atmospheric Research, Boulder, Colorado 80307

INTRODUCTION

Micrometeorologists have traditionally used cup, propeller, and vane anemometers to measure wind speed and direction; sonic anemometers are newer, dating from the 1950s. Today all four types are widely used in research, with cup, propeller, and vane devices also being standard in operational applications.

One early research problem was the measurement of mean wind profiles in the "constant flux" layer, the first few tens of meters above the earth's surface. There the shearing stress τ varies little with height, so its value several meters above the surface can be taken as the surface stress τ_0, which is a scaling parameter for surface-layer structure but also represents the drag on the atmosphere and hence has a strong influence on global circulation. Direct measurements of τ were not possible until fairly recently, but at that time it was known that near the surface the vertical gradient of the mean wind speed U varies as

$$\frac{\partial U}{\partial z} = \frac{1}{kz}\sqrt{\frac{\tau_0}{\rho}} = \frac{u_*}{kz}, \tag{1}$$

where ρ is the density, u_* is the friction velocity, and $k{\sim}0.4$ is the von Kármán constant. Thus (1) was used to deduce τ_0 from mean wind-profile measurements.

Surface-layer researchers subsequently attempted to measure τ directly. Above the surface, τ is represented by the turbulent momentum flux $\rho\langle u_1 u_3\rangle$, where u_1 and u_3 are wind fluctuations in the streamwise and vertical directions and the angle brackets represent an average.

According to Kaimal (1979) the first direct measurements of $\rho\langle u_1 u_3\rangle$ were made in 1926 by F. J. Scrase; soon after, the direct measurement of fluxes of momentum, heat, and moisture in the atmospheric boundary layer (ABL) became a central research goal in micrometeorology. Today, researchers routinely measure these fluxes with various combinations of cup, propeller, vane, and sonic anemometry together with turbulent temperature and humidity sensors.

The scope of micrometeorological research has broadened considerably in the past two decades, and now the ABL is a recognized focus of turbulence research. In a normal day over land the ABL ranges through shear-driven, convectively driven, and stably stratified states, each having different structure and dynamics; this provides turbulence research opportunities not readily available in laboratory flows.

With the discovery of the ABL by the turbulence community have come renewed attempts to use the hot-wire anemometer. However, the excellent spatial and temporal resolution of the hot wire is not generally needed except for dissipative range measurements, and its inherent sensitivity to temperature can be a severe drawback in the relatively low-speed ABL flows. Thus cup, propeller, vane, and sonic anemometers remain the principal types used in ABL research applications.

While the static, or steady-flow, performance of rotating anemometers is now well understood, their dynamic response, more important in turbulence research, is not. Space does not permit an exhaustive review such as that done by Corrsin (1963) on laboratory anemometry, and so I will concentrate on the dynamical aspects here, emphasizing the dynamical nonlinearities, which, while not yet well explored, are particularly important in turbulence research.

CUP ANEMOMETERS

Some Response Considerations

Early studies of cup anemometers dealt with their behavior in steady, nonturbulent flow. Patterson (1926) gave an interesting account of early attempts to calculate the ratio of wind speed to cup speed, called the "factor"; it was taken as three by Robinson, the designer in 1846 of the unit in most common use 80 years later. Patterson attempted to calculate the factor from his extensive wind-tunnel measurements of the torque on stationary and moving cups. In spite of his prodigious effort, however, the agreement between his calculations and the observed factors was only fair.

Researchers turned their attention to cup-anemometer dynamics when it was discovered that they "overspeed," or indicate erroneously high

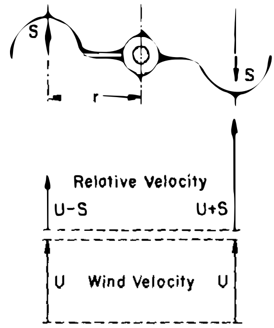

Figure 1 Schematic plan view of a segment of an opposed-cup rotor.

mean values in gusty winds. We will illustrate this and other important aspects of cup-anemometer dynamics through a crude model.

Figure 1 shows a segment of an opposed-cup rotor at an instant when the cup arms are perpendicular to the wind direction. Let c_d and C_d be the drag coefficients of the front and rear cup faces, A the cup area normal to the wind, and let the air and cup speeds be $\mathcal{U}=U+u$ and $\mathcal{S}=S+s$, the sum of mean and fluctuating parts. Then the torque T is

$$T=\frac{\rho Ar}{2}\left[C_d(U+u-S-s)^2-c_d(U+u+S+s)^2\right]. \tag{2}$$

Patterson (1926) and later researchers have shown that T actually varies strongly with angular position; however, for our purely illustrative purposes in this section we will neglect this angular dependence and assume that (2) represents the torque averaged over the basic period of cup rotation.

In a steady wind of speed U with $u=0$, the torque vanishes (for a frictionless rotor) and the anemometer rotates steadily at peripheral speed $S=KU$ with $s=0$; K, the factor, is typically 0.3. Equation (2) gives for this steady case

$$C_d(U^2-2US+S^2)=c_d(U^2+2US+S^2). \tag{3}$$

Equations (2) and (3) can be combined to give

$$T=\frac{2\rho rC_dAKU^2}{(1+K)^2}\times\left[(1-K^2)\frac{u}{U}-(1-K^2)\frac{s}{S}+\left(\frac{u}{U}\right)^2+K^2\left(\frac{s}{S}\right)^2-(1+K^2)\frac{s}{S}\frac{u}{U}\right]. \tag{4}$$

Some of the nonlinear features of cup-anemometer dynamics are apparent from (4). Consider, for example, the initial response to a sudden change u in wind speed, with the anemometer initially in equilibrium so that $s=0$. Then from (4) we have (with I the polar moment of inertia)

$$\frac{I}{r}\frac{ds}{dt}=T=\frac{2\rho r C_d AKU^2}{(1+K)^2}\left[(1-K^2)\frac{u}{U}+\left(\frac{u}{U}\right)^2\right]. \tag{5}$$

Equation (5) indicates that for finite-amplitude wind-speed fluctuations the anemometer responds to wind speed increases ($u>0$) faster than it responds to speed decreases. This is observed, and causes a cup anemometer to overspeed.

To examine the influence of anemometer inertia, consider the equation of motion with the crude expression (4) for torque in the limiting case of small fluctuations u and s:

$$\frac{I}{r}\frac{ds}{dt}=\frac{2\rho r C_d AU(1-K^2)}{(1+K)^2}[Ku-s]. \tag{6}$$

We rewrite this in the form

$$\frac{L}{U}\frac{ds}{dt}+s=Ku, \tag{7}$$

where $L=I/\rho r^2 CA$ and C is an effective drag coefficient, which also includes the numerical factors. L has units of length and is called the "distance constant," since for a given anemometer it is fixed unless the air density changes or the speed range is so large that the drag coefficients change. Thus for small fluctuation levels (7) indicates a cup anemometer is a linear first-order system with a time constant τ inversely proportional to mean wind speed:

$$\tau\frac{ds}{dt}+s=Ku. \tag{8}$$

Cup anemometers in the linear limit are observed to follow (8), with the time constant proportional to $I/\rho r^2 AU$ as predicted above.

While they respond primarily to the wind component in the cup plane, most cup anemometers also have a sensitivity to the velocity component perpendicular to the cup plane; we will refer to this as normal velocity sensitivity. This is usually measured by placing the anemometer in a low-turbulence-level wind tunnel operated at a speed U and tilting the anemometer axis away from vertical by an angle θ. Thus the wind speed in the cup plane is $U\cos\theta$, which would be the indicated speed if the anemometer had no normal velocity sensitivity. Figure 2*a* shows test results reported by MacCready (1966) for two cup anemometers; note that both have significant normal velocity sensitivity. The response asymmetry in θ is due to the effects of the anemometer housing. Kondo et al (1971) show similar results.

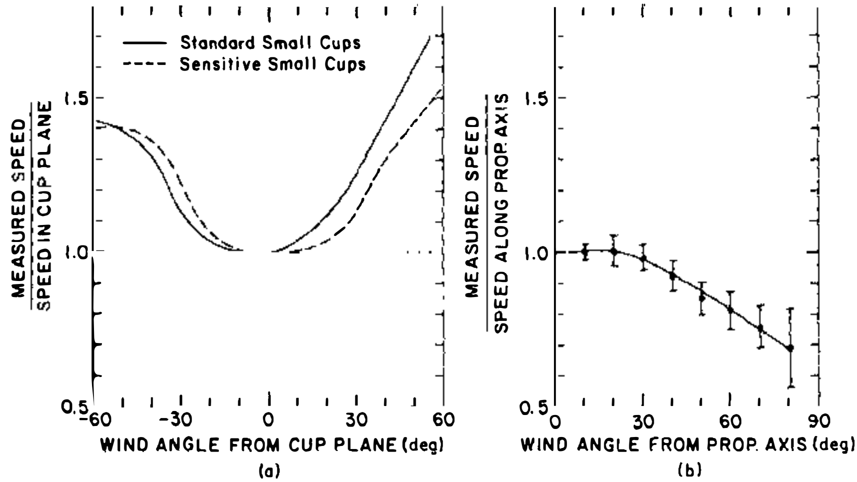

Figure 2 Directional-response characteristics of typical cup and propeller anemometers. (*a*) cup response, from MacCready (1966). (*b*) Gill propeller response, from Pond et al (1979).

The Dynamic Equation

The first published, systematic attempt to develop a finite-amplitude dynamic equation for cup anemometers seems to be that of Schrenk (1929). He noticed that the torque expression for the cup pair in the orientation shown in Figure 1 [our Equation (2)] can be written as

$$\frac{2T}{\rho \mathcal{S}^2 A r} = (C_d - c_d) - 2(C_d + c_d)\frac{\mathcal{U}}{\mathcal{S}} + (C_d - c_d)\left(\frac{\mathcal{U}}{\mathcal{S}}\right)^2. \tag{9}$$

He then assumed that the torque averaged over one cycle also has the form of (9),

$$\frac{2T}{\rho \mathcal{S}^2 A r} = \nu + \mu\left(\frac{\mathcal{U}}{\mathcal{S}}\right) + \lambda\left(\frac{\mathcal{U}}{\mathcal{S}}\right)^2, \tag{10}$$

where ν, μ, and λ are undetermined coefficients. His next and most important step was to measure torque on a rotating cup wheel mounted in a wind-tunnel flow. He then fit the expression (10) to the results in order to evaluate ν, μ, and λ. His results are mainly of historical interest now, since ν, μ, and λ depend on cup-wheel geometry and modern designs are different. However, his approach of directly measuring torque is an excellent technique for developing a dynamic equation for a cup anemometer.

Most other workers have attempted to derive dynamic equations by considering the forces on the individual cups. Some, for example, have started from the Brevoort-Joyner (1934, 1935) data on forces on stationary cups at various angles of incidence. This turns out to be an extraordinarily difficult path to take, in view of the myriad of subtle influences such as cup-wake effects. Ramachandran (1969) and Kondo et al (1971) have proceeded in this way. Acheson (1970) has instead followed Schrenk (1929) and correlated torque measurements with an expression of the form of (10), and Hyson (1972) has used a similar approach.

None of these efforts to develop a dynamic equation has dealt with normal velocity sensitivity, which judging from the data in Figure 2*a* should be important in cup-anemometer dynamics. In fact, Hyson (1972) concludes that the horizontal wind contribution to overspeeding in typical applications is only about 1%, so that if larger values of overspeeding occur they probably are due to w-effects.

Wyngaard, Bauman, & Lynch (1974) (hereafter called WBL) derived a general, nonlinear dynamic equation, which includes normal velocity sensitivity. Their approach is similar to Schrenk's in that it involves torque measurements on a rotating wheel, but their derivation of the dynamic equation from these measurements proceeds somewhat differently.

WBL used the quasi-steady assumption that the smoothed torque $\tilde{T}$ (that is, torque averaged over the basic period of cup rotation) depends only on $\mathfrak{U}$, the vertical velocity $\mathfrak{W}$, and $\mathfrak{S}$. This implies that $\tilde{T}$ is zero under the equilibrium conditions of a steady horizontal wind:

$$\tilde{T}(U_0, 0, S_0) = 0, \tag{11}$$

where the subscript zero denotes the zero-torque condition. Thus WBL expressed $\tilde{T}$ as a three-variable Taylor series expansion about equilibrium:

$$\tilde{T} = \frac{\partial \tilde{T}}{\partial S}\bigg|_0 s + \frac{\partial \tilde{T}}{\partial U}\bigg|_0 u + \frac{\partial \tilde{T}}{\partial W}\bigg|_0 w + \frac{\partial^2 \tilde{T}}{\partial S^2}\bigg|_0 \frac{s^2}{2} + \frac{\partial^2 \tilde{T}}{\partial U^2}\bigg|_0 \frac{u^2}{2} + \frac{\partial^2 \tilde{T}}{\partial W^2}\bigg|_0 \frac{w^2}{2}$$
$$+ \frac{\partial^2 \tilde{T}}{\partial U \partial S}\bigg|_0 us + \frac{\partial^2 \tilde{T}}{\partial U \partial W}\bigg|_0 uw + \frac{\partial^2 \tilde{T}}{\partial S \partial W}\bigg|_0 sw, \tag{12}$$

where w is the vertical velocity fluctuation. Defining $u' = u/U_0$, $s' = s/S_0$, and $w' = w/U_0$ then leads to the dynamic equation

$$s' + \tau \frac{ds'}{dt} = a_1 u' + a_2 w' + a_3 s'^2 + a_4 u'^2 + a_5 w'^2 + a_6 u's' + a_7 u'w' + a_8 s'w', \tag{13}$$

where the time constant $\tau = -I(r\partial\tilde{T}/\partial S|_0)^{-1}$ can be shown to be the usual one having the form L/U_0. The definitions of the dimensionless coefficients a_i follow from (12) and (13) and involve the torque derivatives at equilibrium; they are explicitly given by WBL.

WBL showed that (13) includes, as a special case where $w=0$, the form that follows from the torque expression (10) used by Schrenk. They found that the a_i are subject to the constraints

$$a_1=1; a_3+a_4+a_6=0. \tag{14}$$

They also found that for symmetrical w-response (that is, a response in Figure 2*a* that is even in θ) $a_2=a_7=a_8=0$, and that a_5 can be evaluated from the tilt test used to generate Figure 2*a*.

WBL presented measurements of the a_i based on wind-tunnel measurements of the torque on a rotating cup anemometer. For a standard three-cup anemometer, they found

$$\begin{aligned} a_1 &= 1.03,\\ a_3 &= -0.23,\\ a_4 &= 0.96,\\ a_5 &= 0.67,\\ a_6 &= -0.73, \end{aligned} \tag{15}$$

with the other coefficients zero, within the experimental error. These results (15) are in good agreement with the constraints (14).

The WBL expression (12) for $\tilde{T}$ has all the terms that appeared in the illustrative model (4), but the a_i are different from the coefficients in (4); for example, WBL found a_3 to be negative while (4) indicates it is positive. This suggests the hazards of attempting to derive a response equation through detailed consideration of the complex balance of forces on the rotating, interacting cups rather than measuring torque directly.

The WBL equation for their standard three-cup unit is

$$s'+\frac{\tau ds}{dt}=u'-0.23s'^2+0.96u'^2+0.67w'^2-0.73u's'. \tag{16}$$

The presence of the w'^2 term, which represents normal velocity sensitivity, prevents $s'=u'$ from being a solution, even in the limit of fluctuations so slow that the time-lag term is negligible. In the general case with time lag and finite-amplitude u', s', and w', the form of (16) indicates that nonlinear distortion of s' can occur. We discuss some solutions of (16) in the next section.

Applications to Research

Today's cup anemometers are quite different from those of Schrenk's time. They are also fairly easy to design and build, and many micrometerorologists do so. Examples are described by Jones (1965), Frenzen (1967), and Bradley (1969). Research models tend to have very-low-friction bearings, specially shaped, lightweight cups, and relatively small distance constants [Frenzen (1967) reports values of 0.3–0.6 m, but values for commercial units are typically 2–4 times larger] but can have widely varying normal velocity sensitivity. Frenzen (1967) minimizes this sensitivity with a "staggered six" unit, which has two three-cup wheels separated vertically and offset by 60°; Jones (1965) uses twelve slightly inclined cups. Figure 3 shows two current models of the Argonne

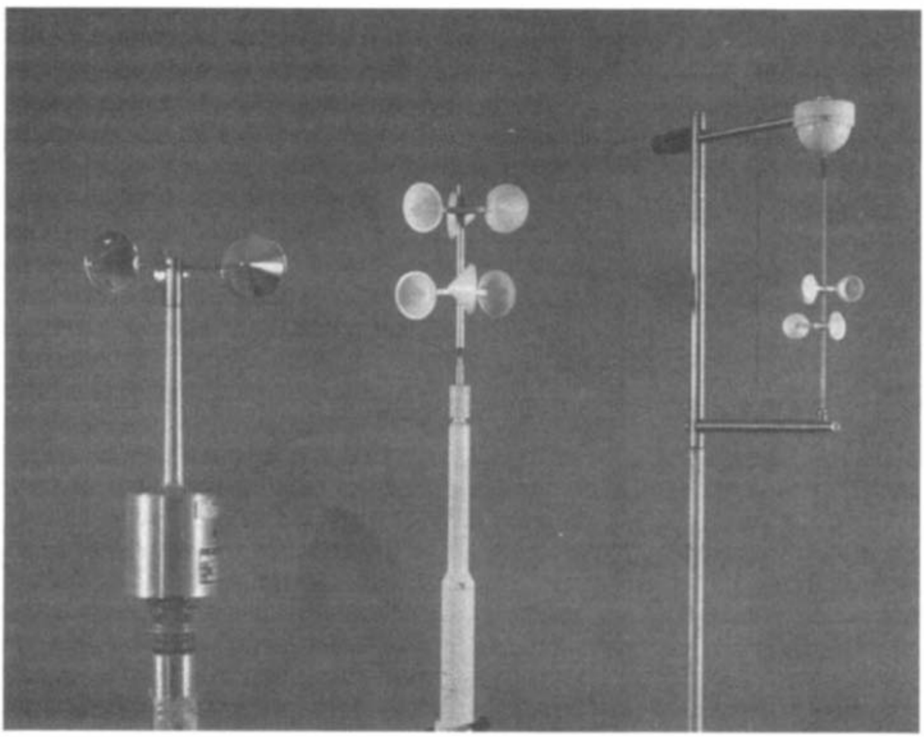

Figure 3 Cup anemometers. *Left*: Weather Measure Model W-1034, with three 5-cm-diameter cups, distance constant 1.5 m. *Center*: Argonne National Laboratory (ANL) low-inertia (LI) model used (in conjunction with w-sensor) for momentum-flux measurements. Six 3.8-cm cups in two-deck array for cosine response; distance constant 0.35 m. *Right*: ANL/LI model for inertial-range measurements; six 2-cm cups, jewel bearings, distance constant 0.25 m. Paul Frenzen photo.

National Laboratory low-inertia cup anemometer and a standard instrument.

The two main research uses for cup anemometers are in mean wind-profile measurements and in turbulence measurements. The principal problem in the first application is overspeeding. If (as is usual) identical cup anemometers are used at different heights, the turbulence characteristics and hence the overspeeding errors will vary with height; thus the measured wind profile can be seriously distorted. To date, overspeeding has been documented primarily through wind-tunnel tests with strongly fluctuating sinusoidal or square-wave winds (Scrase & Sheppard 1944, Deacon 1951), and there is little published, direct evidence of its magnitude in ABL applications, partly because of the lack of another suitable anemometer for comparison. Izumi & Barad (1970) and Högström (1974) each report 10% cup-anemometer overspeeding in different surface-layer experiments, however.

Perhaps the strongest efforts to date to calculate overspeeding in ABL applications are those of Busch & Kristensen (1976) and Kaganov & Yaglom (1976). Each used the WBL response equation (16) for a typical three-cup unit. Busch & Kristensen time-averaged (16) to give an expression for the overspeeding $\langle s' \rangle$:

$$\langle s' \rangle = -0.23\langle s'^2 \rangle + 0.96\langle u'^2 \rangle + 0.67\langle w'^2 \rangle - 0.73\langle u's' \rangle \tag{17}$$

since $\langle u' \rangle = 0$ by definition. They used an approximate analytical technique to evaluate $\langle u's' \rangle$ and $\langle s'^2 \rangle$ and introduced measured wind statistics which enabled them to calculate the overspeeding for various surface-layer conditions. They found that under extreme conditions (a unit with a 20-m distance constant mounted at a height of 2 m over a relatively rough surface in convective conditions) the overspeeding was as large as 30% of the true mean. For a faster (smaller distance constant) unit the overspeeding could be much less. It would be desirable to confirm these results experimentally.

Kaganov & Yaglom (1976) give an exhaustive review of dynamic models, then adopt the WBL form (16) and a perturbation expansion to produce probably the most complete set of response calculations to date. They find overspeeding to be dominated by the normal velocity sensitivity and that it can reach the 10% levels reported by Izumi & Barad (1970) and Högström (1974) in field measurements. They also evaluate approximately the spectral distortion induced by the nonlinearity of the cup-anemometer response.

Like a vertically oriented hot-wire sensor, the cup anemometer responds to the horizontal speed; thus its fluctuating output is only approximately the streamwise wind fluctuation u_1. To illustrate, take an instantaneous anemometer signal that is indicating the instantaneous horizontal speed,

$$\mathcal{U} = U + u = \left[(U_1 + u_1)^2 + u_2^2 \right]^{1/2}, \tag{18}$$

where $(U_1, 0)$ and (u_1, u_2) are the mean and fluctuating horizontal wind vectors. Expanding the right side through second order and averaging gives

$$U = U_1 \left(1 + \frac{\langle u_2^2 \rangle}{2U_1^2} \right), \quad u = u_1 + \frac{U_1}{2} \left[\left(\frac{u_2}{U_1} \right)^2 - \left\langle \left(\frac{u_2}{U_1} \right)^2 \right\rangle \right]. \tag{19}$$

The first equation of (19) indicates the mean error, and the second the contamination of the fluctuating anemometer signal by the fluctuating lateral component. Both effects are also familiar in hot-wire anemometry.

In the linear first-order system approximation, a cup anemometer has a half-power frequency $\omega = U/L$. The distance constant L of research units can be as small as 0.3–0.6 m, giving by Taylor's hypothesis a half-power streamwise wavenumber of $\omega/U = L^{-1} \sim 1.7$–$3.3$ rad m^{-1}, which is typically well into the inertial subrange at heights more than a few meters above the surface. Frenzen (1977) uses the Argonne low-inertia anemometers of Figure 3 for momentum-flux and inertial-subrange measurements.

PROPELLER ANEMOMETERS

Most of today's propeller anemometers have helicoid rotors, and thus derive from the helicoid anemometer first described by W. H. Dines in 1887 (Gill 1973). According to Gill, Dines' anemometer was too complicated for general use and the helicoid was apparently not used again in anemometry until the Bendix Friez Aerovane was developed in the 1940s. In the 1960s Gill and MacCready independently perfected propeller anemometer–bidirectional wind vane units which have been fairly widely adopted.

Today the Gill unit (Holmes et al 1964) is perhaps the most common propeller anemometer used in research. Gill (1975) and Pond et al (1979) discuss its use as a turbulence sensor. Figure 4 shows some models currently manufactured by the R. M. Young Co., of Traverse City, Michigan.

Propeller anemometers, in first approximation, respond linearly to the velocity component normal to the plane of the propeller; we will call this the axial component. The propeller can be flat or helicoid, and most often has two or four blades. The entire unit can be mounted on a vane

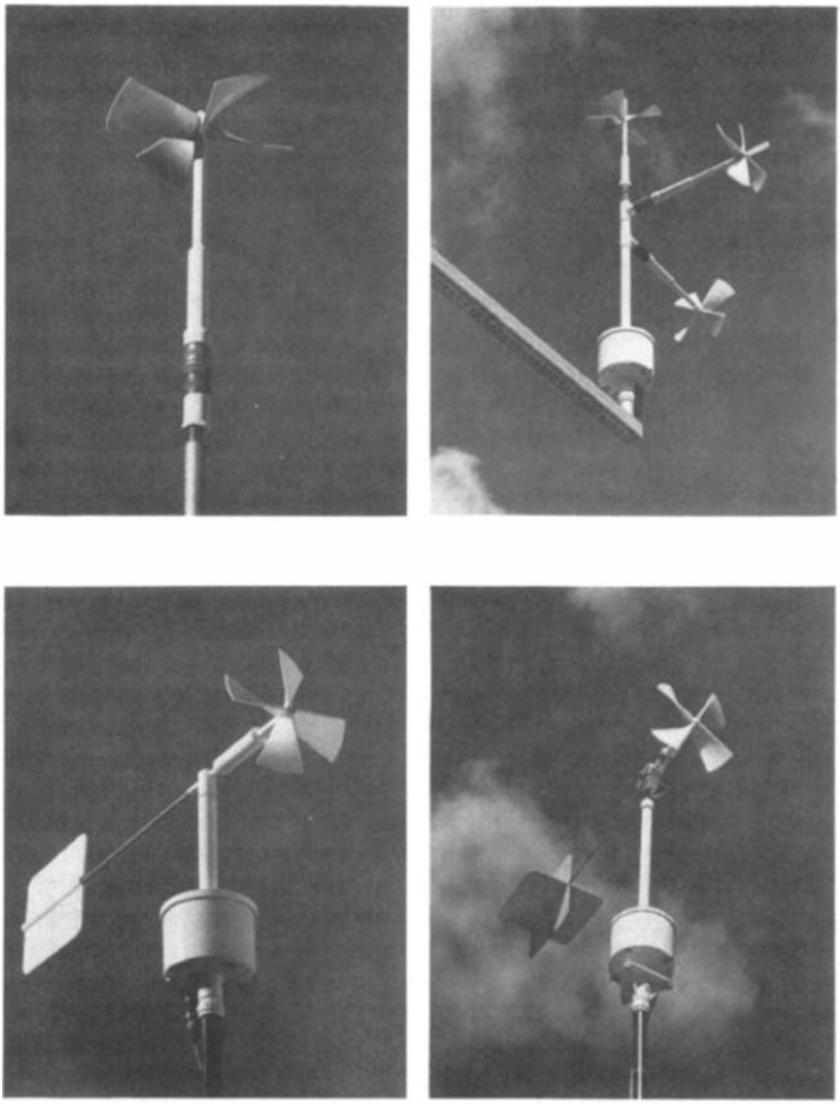

Figure 4 Four R. M. Young Co. Gill propeller anemometers. *Upper left*: vertical-axis unit for measuring vertical velocity. *Upper right*: three-component anemometer. *Lower left*: propeller vane. *Lower right*: Propeller bivane. R. M. Young Co. photos.

to keep the propeller oriented into the wind; this is often preferred, since typical units have significant deviations from axial response. Other workers use fixed units and correct for the actual directional response characteristics.

The propeller anemometer has little competition as an inexpensive, rugged, simple sensor of fluctuating vertical velocity. When combined with sensors for fluctuating streamwise velocity, temperature, or humidity it has made possible the routine measurement of vertical turbulent fluxes. It is not without its idiosyncrasies, but fortunately many of these have been well documented; we will briefly survey the current understanding here. As with cup anemometers, the least-understood area is that of dynamic response.

Directional Sensitivity

The propeller anemometer is, to a fair and widely used approximation, a "cosine-law" device; that is, it responds to $\mathcal{U}\cos\theta$, where $\mathcal{U}$ is the wind speed and θ the angle between the wind and the propeller axis. In their original paper, however, Holmes et al (1964) showed that the measured response departed significantly from cosine behavior. Figure 2*b*, adapted from Pond et al (1979), summarizes some measurements of the directional response of the Gill propeller anemometer. Note that it indicates a speed slower than the axial component, while typical cup anemometers (Figure 2*a*) indicate a speed larger than that in the cup plane. Monna & Driedonks (1979) present data for some other commercial units.

The departures from cosine behavior indicated by Figure 2*b* require correcting in research applications. The R. M. Young Co. boosts the output of its w-sensors by 25% in order to compensate for the decreased sensitivity near 90°, Figure 2*b*. More precise corrections are discussed by Drinkrow (1972) and Horst (1973a).

Frequency Response

A propeller anemometer in an axial wind is usually treated as a first-order linear system with time constant $\tau = L/U$, where L is the distance constant and U the mean wind speed (MacCready & Jex 1964). To first approximation L in axial winds is independent of U, which is why it rather than the time constant is usually quoted. L is of the order of 1 m for four-blade, 23-cm-diameter Gill propeller.

This simple situation changes with off-axis winds, where the time constant is observed to vary with the wind angle (Camp & Turner 1970, Clink 1971, McBean 1972, Horst 1973a, Garratt 1975, Gill 1975, Pond et al 1979). However, in converting measured time constants to distance constants by multiplying by wind speed, some authors use the axial wind-velocity component and others the total wind speed; thus there is some confusion in the literature regarding the value of distance constants for off-axis winds. However, it is clear that for fixed wind speed the propeller time constant increases as θ increases. Garratt (1975), using the data of Hicks (1972), reports that for a Gill propeller the distance constant $U\tau$ (where U is total wind speed) increases from 1.0 m at $\theta=0°$ to about 1.4 m at $\theta=60°$ and then sharply to about 3 m at $\theta=85°$, in fair agreement with the data of Gill (1975). Thus propeller response is much slower when used as a w-sensor (i.e. when the axis is vertical) than when used as a horizontal wind sensor.

Dynamical Response

The propeller anemometer, like the cup anemometer, has inherently nonlinear dynamics. We illustrated the source of cup-anemometer nonlinearity with simple torque arguments based on Figure 1, finding that the responses to finite-amplitude wind-speed increases and decreases were different. A similar analysis of the propeller leads to the same result.

In principle, the propeller anemometer should overspeed, yet there is little reference to this in the literature; however, Brock (1973) has demonstrated propeller-anemometer overspeeding through wind-tunnel tests. Perhaps it is typically less serious than cup-anemometer overspeeding. Wieringa (1972) does mention a cup-anemometer overspeeding correction of 7% applied in a surface-layer experiment and indicates this was determined by comparison with propeller-speed data.

The dependence of the time constant on wind direction is evidence of dynamic nonlinearity of propellers. Further evidence for vertically mounted units is reported by Fichtl & Kumar (1974), who found that the time constant depends on the vertical velocity variance $\langle w^2 \rangle$, and by Francey & Sahashi (1979), who found that the measured power-spectral density of w showed an $f^{-2.5}$ high-frequency falloff rather than the f^{-2} of a first-order linear system. Another nonlinearity is the "dead zone" when used as a w-sensor. An axial wind of the order of 0.2 m s^{-1} is required to overcome starting friction and turn the propeller, and this can cause a loss of small-amplitude w-fluctuations (Wieringa 1972, Horst 1973a).

Acheson (1970) has made one of the few attempts to formulate a nonlinear response equation for propeller anemometers. Adopting the experimental approach used by Schrenk (1929), he measured the torque on units rotating in axial flow in a wind tunnel and found basically the same response equation for cup and propeller anemometers. His solutions for idealized wind forcing and axial flow showed propeller-anemometer overspeeding. The WBL approach, which gives a general, nonlinear response equation for any flow direction, seems yet to be applied to propeller anemometers.

Applications to Research

Propeller anemometers are perhaps the most common sensor for vertical velocity fluctuations and hence for turbulent-flux measurements. Because of their relatively slow w-response, however, they can fail to measure a large fraction of the flux if incorrectly used (McBean 1972, Hicks 1972, Garratt 1975, Kaimal 1975, Francey & Sahashi 1979, Pond et al 1979). Like other sensors, they are prone to vertical misalignment or "tilt," which can introduce spurious horizontal velocity contributions into the vertical velocity signal. Stringent leveling standards are required to minimize this (Pond 1968, Kaimal & Haugen 1969, Wieringa 1972).

In order to eliminate some of the nonlinearities associated with a w-sensing propeller, such as the dead zone and the strongly direction-dependent response time, some researchers prefer to use combinations of inclined units rather than vertical-horizontal arrays. Drinkrow (1972), Horst (1973a), and Pond et al (1979) discuss such applications. It has also been found that a vertical shaft extension on a w-propeller can increase the symmetry of the response (Hicks et al 1977). The same authors (see also Hicks 1972) have discovered that w-propellers are very sensitive to bearing friction, causing the performance as a w-sensor to deteriorate markedly with time. They have also experimented with faster propellers, but find this leads to increased sensitivity to bearing-friction effects.

VANES

Vanes are often used to orient cup, propeller, or hot-wire anemometers into the wind, or used alone to indicate wind direction (see Figure 4). Figure 5 shows miniature vanes used on the NCAR research aircraft. They sense the direction components of the velocity relative to the nose boom (the attack and sideslip angles) to frequencies of 30 Hz at speeds of 70 m s^{-1}; hence, they resolve streamwise wavelengths as small as 2m.

In the schematic of the simple vane of Figure 6 (adapted from Wieringa 1967) the wind vector $\mathcal{U}$ makes an instantaneous angle β to the vane. The vane force acts at the aerodynamic center, a distance r_v from the axis of rotation. The vane velocity at the aerodynamic center is

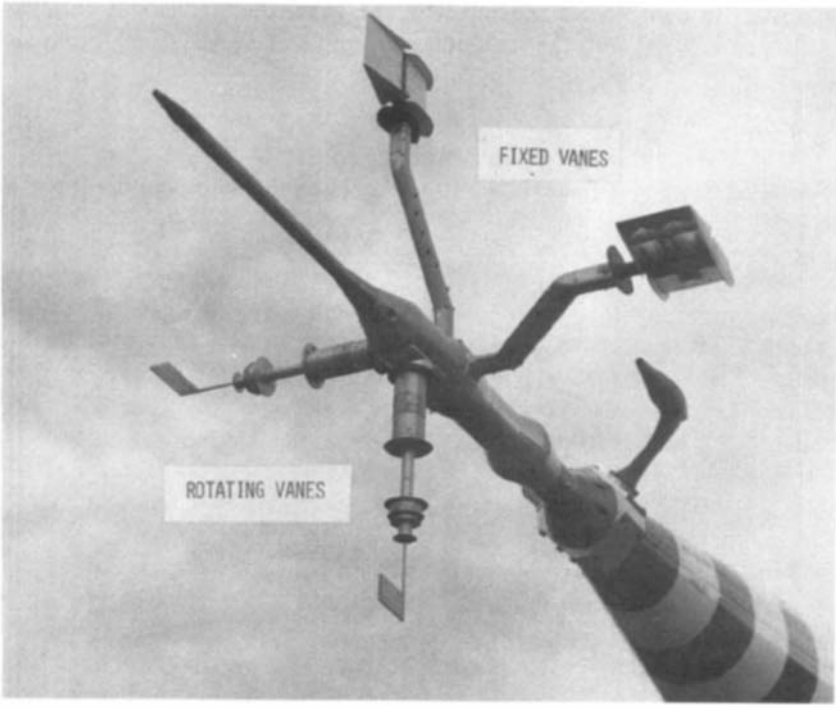

Figure 5 Vanes mounted on a 2-m nose boom on an NCAR Queen Air aircraft. Fixed vanes have 7-cm leading edges, 300-Hz natural frequency; deflection sensed by strain gauges. Rotating vanes are 6.2 × 2.5 cm, 30-Hz natural frequency; position sensed by rotary differential transformer.

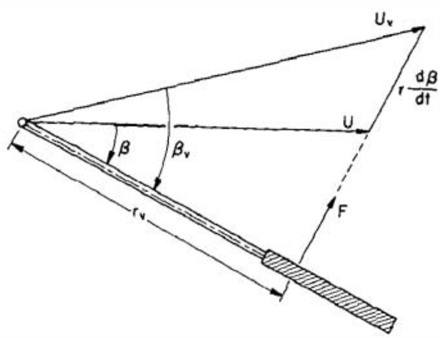

Figure 6 Schematic plan view of a simple vane; adapted from Wieringa (1967).

$r_v d\beta/dt$. In coordinates moving with the vane, the air velocity relative to the vane is $\mathcal{U}_v$ and the instantaneous angle of attack β_v is, for small β,

$$\beta_v \simeq \beta + \frac{r_v}{\mathcal{U}} \frac{d\beta}{dt}. \tag{20}$$

For small β we also have $\mathcal{U}_v = |\mathcal{U}_v| \simeq \mathcal{U}$. Then the aerodynamic force F is

$$F = \frac{\rho \mathcal{U}^2}{2} A C_L \cos\beta_v, \tag{21}$$

where C_L is a lift coefficient and A is the projected vane area in the plane of zero angle of attack. For small β_v,

$$C_L \simeq \left.\frac{\partial C_L}{\partial \beta}\right|_0 \beta_v, \ \cos\beta_v \simeq 1 \tag{22}$$

and the force F and torque T are

$$F \simeq \frac{\rho \mathcal{U}^2}{2} A \left.\frac{\partial C_L}{\partial \beta}\right|_0 \beta_v,$$

$$T \simeq \frac{\rho \mathcal{U}^2}{2} A \left.\frac{\partial C_L}{\partial \beta}\right|_0 r_v\left(\beta + \frac{r_v}{\mathcal{U}} \frac{d\beta}{dt}\right). \tag{23}$$

With respect to a fixed frame of reference, the vane-response equation is then

$$I\frac{d^2\beta}{dt^2} + \frac{\rho}{2}\mathcal{U} A \left.\frac{\partial C_L}{\partial \beta}\right|_0 r_v^2 \frac{d\beta}{dt} + \frac{\rho \mathcal{U}^2}{2} A \left.\frac{\partial C_L}{\partial \beta}\right|_0 r_v(\beta - \phi) = 0, \tag{24}$$

where ϕ is the wind direction. If a parameter N is defined by

$$N = \frac{T}{\beta_v} = \frac{\rho \mathcal{U}^2 A}{2} \left.\frac{\partial C_L}{\partial \beta}\right|_0 r_v \tag{25}$$

then the response equation is simply

$$I\frac{d^2\beta}{dt^2} + \frac{r_v N}{\mathcal{U}} \frac{d\beta}{dt} + N(\beta - \phi) = 0. \tag{26}$$

The vane-response equation (26) is analogous to that for a damped spring-mass system undergoing linear motion. The parameter N is analogous to the spring constant, while $r_v N/\mathcal{U}$ plays the role of the linear damping and I replaces the mass. From (23) and (25) N is the torque, per unit angle of attack, due to static deflection. The remaining torque is due to the vane motion, which causes the relative angle of attack seen by the moving vane to be β_v instead of β; this induces what is called the damping torque. An "aerodynamic damping" D is sometimes defined in the following way:

$$D=\frac{r_{\mathrm{v}}N}{\mathcal{U}}. \tag{27}$$

Thus the equation of vane motion can be written

$$\frac{d^2\beta}{dt^2}+\frac{D}{I}\frac{d\beta}{dt}+\frac{N}{I}(\beta-\phi)=0, \tag{28}$$

which is also expressed as (MacCready & Jex 1964, Acheson 1970)

$$\frac{d^2\beta}{dt^2}+2\zeta\omega_{\mathrm{n}}\frac{d\beta}{dt}+\omega_{\mathrm{n}}^2(\beta-\phi)=0. \tag{29}$$

The natural frequency ω_{n} and damping ζ are, from (25) and (27)–(29),

$$\omega_{\mathrm{n}}=\left(\frac{N}{I}\right)^{1/2}=\left[\frac{\rho\mathcal{U}^2A\left.\frac{\partial C_{\mathrm{L}}}{\partial\beta}\right|_0 r_{\mathrm{v}}}{2I}\right]^{1/2}, \tag{30}$$

$$\zeta=\frac{D}{2(IN)^{1/2}}=\left[\frac{\rho r_{\mathrm{v}}^3A\left.\frac{\partial C_{\mathrm{L}}}{\partial\beta}\right|_0}{8I}\right]^{1/2},$$

from which we see that ω_{n} varies linearly with wind speed $\mathcal{U}$ while ζ is a property of the vane alone, providing that the speed range is small enough that the lift characteristics do not change. Thus we can write ω_{n} as

$$\omega_{\mathrm{n}}=\frac{\mathcal{U}}{\lambda};\quad \lambda=\left[\frac{2I}{\rho A\left.\frac{\partial C_{\mathrm{L}}}{\partial\beta}\right|_0 r_{\mathrm{v}}}\right]^{1/2}, \tag{31}$$

where λ is a natural response length of the vane, independent of the wind speed. The parameter $\lambda_{\mathrm{n}}=2\pi\lambda$ is often called the "natural wavelength."

The vane-response equation (29) is linear for fixed wind speed $\mathcal{U}$, making its solution straightfoward. MacCready & Jex (1964) discuss linear vane response in great detail. Here we simply note that if the wind-angle forcing is a stationary random variable we can write

(Batchelor 1960)

$$\phi(t)=\int e^{i\omega t}\,dE_{\mathrm{in}}(\omega), \tag{32}$$

$$\beta(t)=\int e^{i\omega t}\,dE_{\mathrm{out}}(\omega),$$

and from (29) we have

$$\left(-\omega^2+2i\zeta\omega_{\mathrm{n}}\omega+\omega_{\mathrm{n}}^2\right)dE_{\mathrm{out}}=\omega_{\mathrm{n}}^2\,dE_{\mathrm{in}}. \tag{33}$$

The ratio of input and output power-spectral densities becomes

$$\frac{\Phi_{\mathrm{out}}}{\Phi_{\mathrm{in}}}=\frac{\langle dE_{\mathrm{out}}\,dE_{\mathrm{out}}{}^*\rangle}{\langle dE_{\mathrm{in}}\,dE_{\mathrm{in}}{}^*\rangle}=\frac{1}{\left[1-\left(\frac{\omega}{\omega_{\mathrm{n}}}\right)^2\right]^2+4\zeta^2\left(\frac{\omega}{\omega_{\mathrm{n}}}\right)^2}. \tag{34}$$

If the vane damping is small ($\zeta\ll 1$), (34) indicates the spectral response is sharply peaked for $\omega\sim\omega_{\mathrm{n}}$. MacCready & Jex (1964) show that $\zeta\sim 0.5$–0.7 is optimal, giving a good compromise between fast transient response and smooth spectral response.

In the general case the vane-response equation (29) can be written, by introducing (31),

$$\frac{d^2\beta}{dt^2}+\frac{2\zeta\mathcal{U}}{\lambda}\frac{d\beta}{dt}+\frac{\mathcal{U}^2}{\lambda^2}(\beta-\phi)=0. \tag{35}$$

If $\mathcal{U}$ fluctuates this equation is no longer simple to solve. Such stochastically forced equations are of current interest in their own right, but the only attempts to solve (35) in the context of anemometry seem to be those of Acheson (1970). He used a perturbation expansion to calculate the effects of speed fluctuations on the transfer function, which is (34) in the absence of fluctuations. He found that the fluctuations increased the magnitude of the transfer function at frequencies of the order of ω_{n}. In view of the assumptions made in its derivation, however, it is not clear that (35) is appropriate for studies of vane response to finite-amplitude, three-dimensional turbulence.

The combination of a propeller or cup anemometer and a wind vane is a rather complicated dynamical system, although in the linear limit its response can be analyzed analytically. MacCready & Jex (1964) discuss this in some detail.

Chimonas (1980) describes an interesting application of a simple bivane, which records the instantaneous elevation angle $\phi=\tan^{-1}[(W+w)/(U+u)]$. He shows that when the mean vertical velocity W is negligible the mean elevation angle $\langle\phi\rangle$ is, to second order, simply $\langle uw\rangle/U^2$; hence the bivane could be used to measure Reynolds stress.

Vanes that are constrained from rotating are also used. Lenschow (1971) describes one developed for aircraft mounting; it has faster response than a rotating vane and no bearing friction. Two of these fixed vanes are shown on their aircraft boom in Figure 5. Högström (1967) describes a fixed vane for tower applications.

SONIC ANEMOMETERS

Introduction and History

Sonic (also called acoustic) anemometers, in conjunction with modern developments in data processing and recording, have revolutionized surface-layer turbulence research. To a very accurate approximation a well-designed sonic anemometer measures the projection of the wind-velocity vector on the acoustic path, and is free of the nonlinearities, time lag, and most other deficiencies of cup, propeller, and vane anemometers. Its principal disadvantage is its high cost; a three-component unit is at least an order of magnitude more expensive than a three-component propeller anemometer, for example.

In this section we will briefly review the history and theory of operation of the sonic anemometer. A more complete survey was recently done by Kaimal (1979); much of the material here is taken from his paper.

Suomi (1957) was a pioneer in sonic anemometry. His device had a 1-m path; the transit-time difference of acoustic pulses traveling in opposite directions along this path gave the average velocity along the path direction. Later workers used continuous acoustic signals (Gurvich 1959, Bovsheverov & Voronov 1960, Kaimal & Businger 1963). The 1968 Kansas experiments (Haugen et al 1971, Haugen 1973) saw the first use of sonic anemometry in a large-scale field program. Three-component, pulse-type sonic anemometers with 20-cm paths were used at heights of 5.7, 11.3, and 22.6 m in a study of the structure and dynamics of the surface layer. Kaimal et al (1974) describe an improved device, an updated version of which will soon be commercially available from Applied Technology Corporation of Boulder, Colorado.

Theory of Operation

Figure 7, from Kaimal (1979), shows the basic principle of the sonic anemometer. The wind vector **V** has components V_d and V_n along and normal to the acoustic path, and we assume that all velocities are averages along the paths. The transit times for two simultaneous pulses traveling from T_1 to R_1 and from T_2 to R_2 are, from the vector diagram

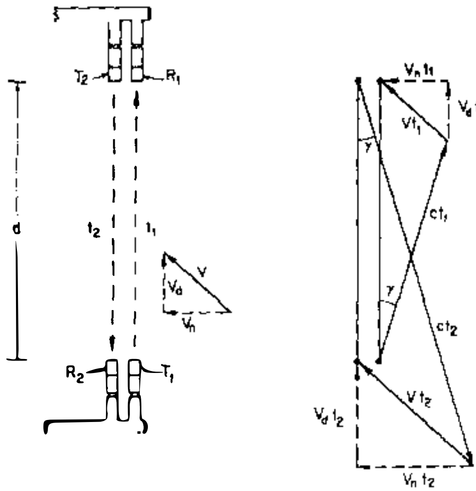

Figure 7 Sound-ray vectors for a single-axis sonic anemometer, showing principle of operation; T and R represent transmitter and receiver, respectively. Adapted from Kaimal (1979).

in Figure 7,

$$t_1 = \frac{d}{c\cos\gamma + V_d}, \tag{36}$$

$$t_2 = \frac{d}{c\cos\gamma - V_d}.$$

Here t_1 and t_2 are the pulse transit times, d is the path length, c is the velocity of the sound in the air, and $\gamma = \sin^{-1}(V_n/c)$. Thus for $V^2 \ll c^2$ the transit-time difference is, from (36),

$$\Delta t = \frac{2d}{c^2} V_d. \tag{37}$$

Knowing the temperature T gives c^2 from the relation $c^2 = kRT$, where k is the ratio of specific heats and R the gas constant. Thus, when T is known, measuring V_d becomes a matter of the measurement of the transit-time difference. For $d = 20$ cm this typically can be done with a resolution of about 10^{-7} s in commercial units, giving a velocity resolution of the order of 3 cm s^{-1}. Kaimal (1979) has discussed the influence of temperature and humidity fluctuations, which affect the sound speed c, on the velocity measurements; they are generally negligible.

Three-Dimensional Units

According to Kaimal (1979), the problem of designing a three-dimensional sonic array with unobstructed exposure for all the axes is not a trivial one. Current models use a pair of horizontal axes separated by 120 degrees and one vertical axis; the three orthogonal velocity components are then retrieved from these outputs. However, the outputs must be monitored to ensure that the natural variations in wind direction do not exceed the allowable range of this array, which is of the order of 90 degrees in the horizontal. Figure 8 shows a three-axis sonic anemometer with 20-cm paths.

Current units with a pair of acoustic paths per axis typically have pulse rates on the order of 400 s^{-1}. Thus Kaimal (1979) points out that 10 or 20 successive measurements can be block-averaged to improve resolution and reduce spectral-aliasing effects, while leaving a signal of the order of 20 samples s^{-1}. Some units use only one transducer at each end of the path, acting alternately as a transmitter and a receiver; here

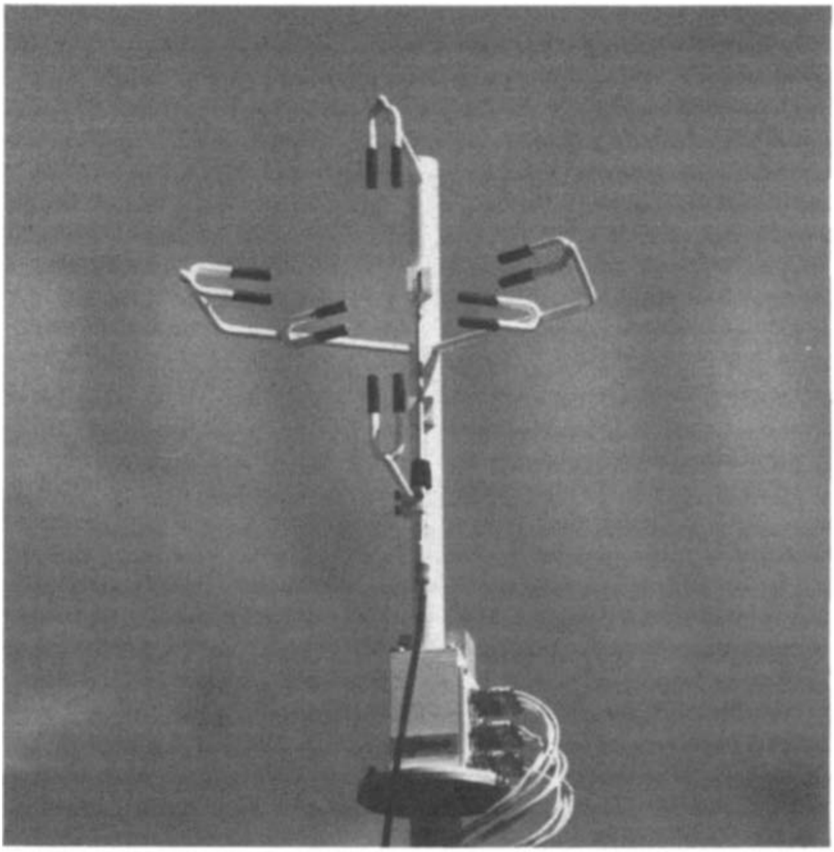

Figure 8 A three-axis sonic anemometer (EG & G model 198-3) with 20-cm paths. J. C. Kaimal photo.

the sample rate must be less (no greater than 10 s^{-1}) to accommodate settling times in the transducers.

The spatial-resolution properties of three-component sonic arrays have been calculated in some detail by Kaimal et al (1968) and by Horst (1973b). They have calculated the effects of path length and path separation on measured horizontal and vertical velocity spectra, assuming the true spectra are inertial and isotropic. Their results indicate that the measured streamwise wavenumber spectra (inferred from frequency spectra through Taylor's hypothesis) of horizontal and vertical velocity components become distorted at streamwise wavenumbers κ_1 of the order of d^{-1}; thus the "distance constant" is effectively the path length, which at typically 20 cm is less than the distance constant of most cup or propeller anemometers. This gives sufficient spatial resolution to recover the vertical turbulent fluxes at heights of the order of 5 m and greater (Kaimal 1975).

Sonic-anemometer velocity measurements can be systematically underestimated because of the velocity defects in the transducer wakes along the acoustic paths. The severity of this effect depends on the array design. Kaimal (1979) cites some calibration data that suggest it could be important in very-short-path arrays, which tend to use transducers of the same diameter as longer-path units. However, there are as yet no published calculations or measurements of the influence of these errors on various turbulence statistics.

Kaimal's (1979) concluding remarks are appropriate here:

> The sonic anemometer with its rapid response, linear output and stable calibration has become a valuable tool for atmospheric research. It has provided high-quality turbulence data in a number of field experiments conducted during the last decade. A new three-axis configuration is currently being used for continuously monitoring the wind at eight levels on the Boulder Atmospheric Observatory's 300 m tower.
>
> Because of its complexity and high cost, the sonic anemometer is likely to remain a research instrument. Attempts are being made to reduce cost and to simplify its operation. Even if these attempts are successful, the sonic anemometer has an inherent limitation which precludes its use in adverse weather conditions. The instrument fails to respond in rain, wet snow, and heavy fog. Formation of water drops on the transducer temporarily affects its operation. Thus the sonic anemometer's main contribution will be in fair-weather observations of atmospheric turbulence, where it is still the instrument of choice among boundary-layer physicists.

SUMMARY

The static response of cup and propeller anemometers to wind speed and direction is generally well understood. Their dynamic response can be broadly described in linear terms, but a full description requires nonlinear models. Much progress has been made in the last decade in

formulating and studying nonlinear models of cup anemometers, but the extension to propellers has not been carried out although it is straightforward. There is little published work on the nonlinear dynamics of vanes.

Further studies of the nonlinear dynamics of cup, propeller, and vane anemometers would be most useful, particularly as researchers probe more deeply into ABL turbulence structure and require increasing fidelity from these commonly used sensors.

Sonic-anemometer response is inherently linear and hence better understood. The effect of temperature and water-vapor fluctuations on its measured velocities is well documented and generally negligible, and its spatial-resolution characteristics have been calculated in great detail. A remaining problem that deserves more attention is the influence of the transducer wakes on the measured velocities.

ACKNOWLEDGMENTS

I am grateful to D. Acheson, F. Bradley, S. Corrsin, and J. C. Kaimal for a number of stimulating discussions on anemometry over the past decade. H. Baynton, F. Brock, P. Frenzen, J. C. Kaimal, D. Kipley, and D. Lenschow have been very helpful during the preparation of this review. Finally, I wish to thank P. Waukau for expertly typing several drafts of this manuscript. The National Center for Atmospheric Research is sponsored by the National Science Foundation.

Literature Cited

Acheson, D. T. 1970. Response of cup and propellor rotors and wind direction vanes to turbulent wind fields. *Meteorol. Monogr.* 11:252–61

Batchelor, G. K. 1960. *The Theory of Homogeneous Turbulence*. Cambridge Univ. Press. 197 pp.

Bovsheverov, V. M., Voronov, V. P. 1960. Acoustic anemometer. *Izv. Geophys. Series*. 6:882–85

Bradley, E. F. 1969. A small sensitive anemometer system for agricultural meteorology. *Agric. Meteorol.* 6:185–93

Brevoort, M. J., Joyner, U. T. 1934. Aerodynamic characteristics of anemometer cups. *NACA Tech. Note No. 489*

Brevoort, M. J., Joyner, U. T. 1935. Experimental investigation of the Robinson-type cup anemometer. *NACA Rep. No. 513.* 24 pp.

Brock, F. 1973. *Experimental analysis of propeller anemometer dynamic performance*. PhD thesis. Univ. Okla., Norman. 71 pp.

Busch, N. E., Kristensen, L. 1976. Cup anemometer overspeeding. *J. Appl. Meteorol.* 15:1328–32

Camp, D. W., Turner, R. E. 1970. Response tests of cup, vane, and propeller wind sensors. *J. Geophys. Res.* 75:5265–70

Chimonas, G. 1980. Reynolds stress deflections of the bivane anemometer. *J. Appl. Meteorol.* 19:329–33

Clink, W. L. 1971. Comment on "Response tests of cup, vane, and propeller wind sensors" by D. W. Camp, R. E. Turner, and L. P. Gilchrist. *J. Geophys. Res.* 76:2902

Corrsin, S. 1963. Turbulence: Experimental Methods. In *Handbuch der Physik*, ed. S. Flugge, C. Truesdell. 8(2):524–90. Berlin: Springer

Deacon, E. L. 1951. The over-estimation error of cup anemometers in fluctuating winds. *J. Sci. Instrum.* 28:231–34

Drinkrow, R. 1972. A solution to the paired Gill-anemometer response function. *J.*

Appl. Meteorol. 11:76–80

Fichtl, G. H., Kumar, P. 1974. The response of a propeller anemometer to turbulent flow with the mean wind vector perpendicular to the axis of rotation. *Boundary-Layer Meteorol.* 6:363–79

Francey, R. J., Sahashi, K. 1979. Gill propeller anemometer frequency response over the sea. *J. Appl. Meteorol.* 18:1083–86

Frenzen, P. 1967. Modifications of cup anemometer design to improve the measurement of mean horizontal wind speeds in turbulence. *Ann. Rep. Radiol. Phys. Div.*, Argonne Nat'l. Lab., *ANL-7360*, pp. 160–66

Frenzen, P. 1977. A generalization of the Kolmogorov–von Kármán relationship and some further implications on the values of the constants. *Boundary-Layer Meteorol.* 11:375–80

Garratt, J. R. 1975. Limitations of the eddy-correlation technique for the determination of turbulent fluxes near the surface. *Boundary-Layer Meteorol.* 8:255–59

Gill, G. C. 1973. The helicoid anemometer. *Atmosphere* 11:145–55

Gill, G. C. 1975. Development and use of the Gill UVW anemometer. *Boundary-Layer Meteorol.* 8:475–95

Gurvich, A. S. 1959. Acoustic microanemometer for investigation of the microstructure of turbulence. *Acoustic J.* (USSR) 5:368–69

Haugen, D. A., ed. 1973. *Workshop on Micrometeorology*, Am. Meteorol. Soc., Boston. 300 pp.

Haugen, D. A., Kaimal, J. C., Bradley, E. F. 1971. An experimental study of Reynolds stress and heat flux in the atmospheric surface layer. *Q. J. R. Meteorol. Soc.* 97:168–80

Hicks, B. B. 1972. Propeller anemometers as sensors of atmospheric turbulence. *Boundary-Layer Meteorol.* 3:214–28

Hicks, B. B., Frenzen, P., Wesely, M. L. 1977. Some preliminary results from the 1976 ITCE: I. Anemometry. *Ann. Rep., Radiol. & Environ. Res. Div.*, Argonne Nat'l Lab., *ANL-76-88*, pp. 127–32

Högström, U. 1967. A new sensitive eddy flux instrumentation. *Tellus* 19:230–39

Högström, U. 1974. A field study of the turbulent fluxes of heat, water vapour and momentum at a "typical" agricultural site. *Q. J. R. Meteorol. Soc.* 100: 624–39

Holmes, R. M., Gill, G. C., Carson, H. W. 1964. A propellor-type vertical anemometer. *J. Appl. Meteorol.* 3:802–4

Horst, T. W. 1973a. Corrections for response errors in a three-component propeller anemometer. *J. Appl. Meteorol.* 12:716–25

Horst, T. W. 1973b. Spectral transfer functions for a three-component sonic anemometer. *J. Appl. Meteorol.* 12:1072–75

Hyson, P. 1972. Cup anemometer response to fluctuating wind speeds. *J. Appl. Meteorol.* 11:843–48

Izumi, Y., Barad, M. L. 1970. Wind speeds as measured by cup and sonic anemometers and influenced by tower structure. *J. Appl. Meteorol.* 9:851–56

Jones, J. I. P. 1965. A portable sensitive anemometer with proportional d.c. output and a matching wind velocity-component resolver. *J. Sci. Instrum.* 42:414–17

Kaganov, E. I., Yaglom, A. M. 1976. Errors in wind-speed measurements by rotation anemometers. *Boundary-Layer Meteorol.* 10:15–34

Kaimal, J. C. 1975. Sensors and techniques for direct measurement of turbulent fluxes and profiles in the atmospheric surface layer. *Atmos. Tech.* 7:7–14. Available from NCAR, P. O. Box 3000, Boulder, Colorado 80307

Kaimal, J. C. 1979. Sonic anemometer measurement of atmospheric turbulence. *Proc. Dynamic Flow Conf., 1978*, pp. 551–65. P. O. Box 121, DK 2740 Skovlunde, Denmark

Kaimal, J. C., Businger, J. A. 1963. A continuous wave sonic anemometer thermometer. *J. Appl. Meteorol.* 2:156–64

Kaimal, J. C., Haugen, D. A. 1969. Some errors in the measurement of Reynolds stress. *J. Appl. Meteorol.* 8:460–62

Kaimal, J. C., Newman, J. T., Bisberg, A., Cole, K. 1974. An improved three-component sonic anemometer for investigation of atmospheric turbulence. In *Flow—Its Measurement and Control in Science and Industry* Vol. 1, pp. 349–59. Instrum. Soc. Amer.

Kaimal, J. C., Wyngaard, J. C., Haugen, D. A. 1968. Deriving power spectra from a three-component sonic anemometer. *J. Appl. Meteorol.* 7:827–37

Kondo, J., Naito, G., Fujinawa, Y. 1971. Response of cup anemometer in turbulence. *J. Meteorol. Soc. Japan.* 49:63–74

Lenschow, D. H. 1971. Vanes for sensing incidence angles of the air from an aircraft. *J. Appl. Meteorol.* 10:1339–43

MacCready, P. B. 1966. Mean wind speed measurements in turbulence *J. Appl.*

Meteorol. 5:219–25

MacCready, P. B., Jex, H. R. 1964. Response characteristics and meteorological utilization of propeller and vane wind sensors. *J. Appl. Meteorol.* 3:182–93

McBean, G. A. 1972. Instrument requirements for eddy correlation measurements. *J. Appl. Meteorol.* 11:1078–84

Monna, W. A. A., Driedonks, A. G. M. 1979. Experimental data on the dynamic properties of several propeller vanes. *J. Appl. Meteorol.* 18:699–702

Patterson, J. 1926. The cup anemometer. *Trans. R. Soc. Can.* Ser. III, 20:1–54

Pond, S. 1968. Some effects of buoy motion on measurements of wind speed and stress. *J. Geophys. Res.* 73:507–12

Pond, S., Large, W. G., Miyake, M., Burling, R. W. 1979. A Gill twin propeller-vane anemometer for flux measurements during moderate and strong winds. *Boundary-Layer Meteorol.* 16:351–64

Ramachandran, S. 1969. A theoretical study of cup and vane anemometers. *Q. J. R. Meteorol. Soc.* 95:163–80

Schrenk, O. 1929. Uber die Trägheitsfehler des Schalenkreuz-Anemometers bei schwankender Windstärke. *Z. Tech. Phys.* 10:57–66

Scrase, F. J., Sheppard, P. A. 1944. The errors of cup anemometers in fluctuating winds. *J. Sci. Instrum.* 21:160–61

Suomi, V. E. 1957. Sonic anemometer. In *Exploring the Atmosphere's First Mile,* 1:356–66. New York: Pergamon

Wieringa, J. 1967. Evaluation and design of wind vanes. *J. Appl. Meteorol.* 6:1114–22

Wieringa, J. 1972. Tilt errors and precipitation effects in trivane measurement of turbulence fluxes over open water. *Boundary-Layer Meteorol.* 2:406–26

Wyngaard, J. C., Bauman, J. T., Lynch, R. A. 1974. Cup anemometer dynamics. See Kaimal et al 1974, pp. 701–8